



OPEN

# Identification and optimization of the key growth parameters involved in carotenoids production of the marine microalga *Pavlova gyrans*

Filipe Maciel<sup>1,2</sup>, Paulo Berni<sup>1,2</sup>, Pedro Geada<sup>1,2</sup>✉, José Teixeira<sup>1,2</sup>, Joana Silva<sup>3</sup> & António Vicente<sup>1,2</sup>

In this work, a multivariate analysis was carried out, using a Plackett–Burman (PB) design involving seventeen growth parameters, on carotenoids production of *Pavlova gyrans* ( $p < 0.10$ ). Each assay was analysed regarding its content ( $\text{mg g}^{-1}$ ) of fucoxanthin (Fx), diatoxanthin, diadinoxanthin,  $\beta$ -carotene ( $\beta\text{Car}$ ),  $\alpha$ -carotene, and the sum of all carotenoids analysed individually (TCar). According to the statistical analysis, modified medium formulations were developed for the particular cases of Fx,  $\beta\text{Car}$ , and TCar. The study showed that Fx content was positively affected by nitrogen supplementation and lower light intensities. Higher concentrations of nitrogen and iron increased the final content of  $\beta\text{Car}$  as well. Similarly, salinity, light intensity, nitrogen, iron, and cobalt were identified as key factors in TCar production. The PB-based formulations showed significant improvements ( $p < 0.05$ ) for TCar ( $11.794 \text{ mg g}^{-1}$ ) and Fx ( $6.153 \text{ mg g}^{-1}$ ) when compared to the control conditions (Walne's medium— $2.010 \text{ mg g}^{-1}$ ). Furthermore, effective control of key variables (e.g., light intensity) throughout *P. gyrans* growth proved successful ( $p < 0.05$ ), increasing the productivity of Fx ( $0.759 \text{ mg L}^{-1} \text{ d}^{-1}$ ) and TCar ( $1.615 \text{ mg L}^{-1} \text{ d}^{-1}$ ).

Carotenoids are the pigments responsible for the yellow, orange, and red colors in nature, such those presented by microalgae, bacteria, and plants<sup>1</sup>. They have been highlighted as high added-value products due to their biological activity and coloring properties, which make them of great interest for biotechnological and industrial applications<sup>2</sup>. Most of these functions are associated with the antioxidant properties of carotenoids due to their ability to quench singlet oxygen and reactive oxygen species, which is strongly dependent of the pigments' chemical composition<sup>3,4</sup>.

Humans are not able to naturally synthesize carotenoids and their needs are only met through proper nutrition. Thus, considering their biological relevance along with the consumers' awareness for a healthy lifestyle, there has been an increasing demand for carotenoids in recent decades, estimating a compound annual growth rate of 5.7% and a potential global market value of 2.7 billion US\$ by 2027<sup>5</sup>. Cheaper production of chemically synthesized colorants makes them attractive, however, they represent a high environmental impact and health concerns raised when used as ingredient for human consumption<sup>6</sup>. Furthermore, synthetic carotenoids are not a viable option since they have significantly lower bioactivity compared to the natural ones<sup>7</sup>.

Microalgae have been presented as one of the most promising alternative sources of natural carotenoids. These microorganisms are widespread in nature and are known for their high photosynthetic activity, fast growth, and metabolic plasticity. They possess a rich composition, which can include several bioactive pigments, polyunsaturated fatty acids and/or high protein content<sup>8–10</sup>. Several species have been commercially explored as producers of carotenoids, being the most well-known examples *Haematococcus pluvialis* and *Dunaliella salina*, which can produce 6% and 10% of their dry weight (DW) as astaxanthin and  $\beta\text{Car}$ , respectively<sup>11,12</sup>.

Nevertheless, the differentiated properties of natural carotenoids, along with challenging implementation of microalgae production at industrial scale, contributed to their increasing market value, which can reach 1500

<sup>1</sup>CEB - Centre of Biological Engineering, University of Minho, Campus de Gualtar, Braga, Portugal. <sup>2</sup>LABELLS - Associate Laboratory, Braga, Guimarães, Portugal. <sup>3</sup>ALLMICROALGAE, Natural Products S.A., Lisbon, Portugal. ✉email: pedrogeada@ceb.uminho.pt

US\$ kg<sup>-1</sup> for  $\beta$ Car or even 42,000 US\$ kg<sup>-1</sup> for Fx<sup>13</sup>. Thus, to improve the cost-effectiveness of the process, several research studies have been carried out with the aim of identifying microalgae species enriched in carotenoids and evaluating growth conditions and strategies to improve biomass production and carotenoids accumulation<sup>14,15</sup>.

Recently, microalgae from the Pavlovophyceae class have been seen as a promising source of bioactive compounds for industries other than aquaculture, such as food and pharmaceutical industries or even wastewater management<sup>16–19</sup>. Firstly, its commercial interest relied on their ability to produce large lipids contents enriched with the high valuable eicosapentaenoic acid (EPA) and docosahexaenoic acid (DHA)<sup>20</sup>. However, these microalgae also present an interesting composition of sterols, essential amino acids, higher digestibility due to the absence of cell wall and a valuable carotenoids profile composed of diadinoxanthin (Ddx), diatoxanthin (Dtx),  $\beta$ Car and, mostly, Fx (51–68% of total carotenoids)<sup>18,20,21</sup>. As previously mentioned, carotenoids have been highlighted and highly demanded due to their biological properties. Among them, Fx has shown enormous potential and interest for the nutraceutical market given its differentiated and high bioactivity, such as anti-obesity<sup>22</sup>, anti-cancer<sup>23</sup>, and anti-diabetic effect<sup>24</sup>.

The present study aims to optimize the carotenoids accumulation of the microalga *Pavlova gyrans* through a multivariate approach involving seventeen growth parameters. As described in Maciel, F. et al<sup>25</sup>, three abiotic factors stood out among seventeen as the most significant for the growth of *P. gyrans*: light intensity, NaNO<sub>3</sub> and CuSO<sub>4</sub>·5H<sub>2</sub>O. These three variables, together with phosphorus, were optimised, showing a 3.8-fold increase in biomass production. The optimal combination obtained validates the positive effect of greater irradiation and nitrogen and phosphorus supplementation, while copper promoted superior growth when supplied in lower concentrations<sup>25</sup>. To the authors' knowledge, and unlike other haptophytes (e.g. *Tisochrysis lutea*) and diatoms (e.g. *Phaeodactylum tricorutum*), few studies were found that include the simultaneous study of a large number of growth conditions on carotenoids content—and, in particular, on Fx—of Pavlovophyceae species, despite their potential as carotenoids source. Throughout the optimization process, several growth conditions were formulated and validated against the control conditions. Moreover, the most significant growth parameters were also validated against the optimum growth conditions for biomass production of *P. gyrans*, which were determined in a previous work of our research group<sup>25</sup>.

## Material and methods

### Microalga and inoculum preparation

The non-axenic microalga strain *Pavlova gyrans* (RCC1553) was obtained from the Roscoff Culture Collection (Roscoff, France). It was maintained in Walne's medium (500 mg L<sup>-1</sup> NaNO<sub>3</sub>), at Level 0 (Table 1), under salinity of 30 psu<sup>26</sup>. The inoculum was up-scaled to 2 L flat bottom flask, in which was bubbled with a mixture of air and CO<sub>2</sub> (8 mL min<sup>-1</sup>—Alicat Scientific, USA) to keep the pH value in the range of 8.0 ± 0.5. The cultures were grown at room temperature (22 to 26 °C) and laterally irradiated with white light emitting diodes (LEDs—100  $\mu$ mol photons m<sup>-2</sup> s<sup>-1</sup>) over 24 h. Photosynthetically active radiation (PAR) was measured with a Li-250A light meter equipped with Q44069 sensor.

Abiotic factor		Level		
		- 1	0	1
$x_1$	Inoculum size (AFDW g L <sup>-1</sup> )	0.1	0.2	0.3
$x_2$	Salinity (psu)	20	30	40
$x_3$	Light intensity ( $\mu$ mol photons m <sup>-2</sup> s <sup>-1</sup> )	150	450	750
$x_4$	Air flow (mL min <sup>-1</sup> )	600	800	1000
$x_5$	NaNO <sub>3</sub> (mg L <sup>-1</sup> )	250	500	750
$x_6$	NaH <sub>2</sub> PO <sub>4</sub> H <sub>2</sub> O (mg L <sup>-1</sup> )	10	20	30
$x_7$	Na <sub>2</sub> H <sub>2</sub> EDTA 2H <sub>2</sub> O (mg L <sup>-1</sup> )	22.5	45	67.5
$x_8$	H <sub>3</sub> BO <sub>3</sub> (mg L <sup>-1</sup> )	16.8	33.6	50.4
$x_9$	FeCl <sub>3</sub> 6H <sub>2</sub> O (mg L <sup>-1</sup> )	0.65	1.3	1.95
$x_{10}$	MnCl <sub>2</sub> 4H <sub>2</sub> O ( $\mu$ g L <sup>-1</sup> )	180	360	540
$x_{11}$	NaHCO <sub>3</sub> (mg L <sup>-1</sup> )	170	652	1134
$x_{12}$	ZnCl <sub>2</sub> ( $\mu$ g L <sup>-1</sup> )	10.25	21	31.75
$x_{13}$	CoCl <sub>2</sub> 6H <sub>2</sub> O ( $\mu$ g L <sup>-1</sup> )	10	20	30
$x_{14}$	(NH <sub>4</sub> ) <sub>6</sub> Mo <sub>7</sub> O <sub>24</sub> 4H <sub>2</sub> O ( $\mu$ g L <sup>-1</sup> )	4.5	9	13.5
$x_{15}$	CuSO <sub>4</sub> 5H <sub>2</sub> O ( $\mu$ g L <sup>-1</sup> )	10	20	30
$x_{16}$	Thiamin ( $\mu$ g L <sup>-1</sup> )	50	100	150
$x_{17}$	Cyanocobalamin ( $\mu$ g L <sup>-1</sup> )	2.5	5	7.5

**Table 1.** The seventeen abiotic factors, and respective levels, assessed in the carotenoids composition of *P. gyrans* through the Plackett–Burman experimental design.

## Screening of the growth parameters for carotenoids production by *P. gyrams* using a Plackett–Burman design

The experimental design adopted to assess the impact of growth factors on the carotenoids composition of *P. gyrams* comprise the experiments performed in Maciel, F. et al.<sup>25</sup>, Table 1. Each factor was evaluated at three different levels: -1, 0, and 1. The corresponding combinations of the growth conditions are presented in Table 2. Briefly, seventeen growth parameters were assessed through a Plackett–Burman design (PB), composed of 24 individual combinations and 4 central points (assays 25–28), totaling 28 assays<sup>27</sup>. All independent variables were set at Level 0 in the central points, which allowed evaluating the repeatability of the carotenoids' composition of *P. gyrams*. The experiments were carried out randomly in three separated experimental runs, using 1 L bubble column reactors (glass, 6.5 cm diameter and 43 cm high—see supplementary material) at room temperature and laterally illuminated with LEDs lighting. Salinity was adjusted using a concentrated sea salt stock solution and measured with a seawater refractometer (Hanna HI 96,822, USA). Reactors were continuously aerated with filtered air (0.2 µm) through an internal glass tube located at the center of the reactor. CO<sub>2</sub> was supplied in-line (0.6 mL min<sup>-1</sup>) to keep pH = 8.0 ± 0.5 (Hanna HI 2210, USA).

Microalgal growth was monitored by optical density (750 nm) every 2 days, being this value subsequently converted to ash-free dry weight (AFDW) using the following calibration curve:  $AFDW(g L^{-1}) = 0.8991 \times OD_{750} + 0.0054$ ,  $R^2 = 0.99$ . The experiments were stopped once the stationary growth phase was attained and the cultures were centrifuged at 2147 g for 20 min (Centurion Pro-Analytical CR7000, Chichester, United Kingdom). The pellets were recovered and stored at -20 °C, and further at -80 °C for lyophilization.

### Validation test

The calculated effects and corresponding statistical significance of the PB design enabled the identification of the most relevant growth conditions for each carotenoid assessed and the sum of all carotenoids (mg g<sup>-1</sup>) in *P. gyrams*. That information was used to define tailored growth conditions for the carotenoid of interest, in which the carotenoids' yields were evaluated and validated in two new different sets of experiments (V1 and V2). The full composition of the growth conditions used in both sets of experiments is described in Table 3. The first set (V1) aimed at validating the optimum conditions defined in PB design for the dependent variables Fx, TCar, and βCar, against the control conditions (Con—Walne's medium). For practical reasons, the variables inoculum size ( $x_1$ ), light intensity ( $x_3$ ), and air flow ( $x_4$ ) in the control assay were the same of the remaining experiments. The non-significant growth parameters factors ( $p > 0.10$ ) for Fx, βCar and TCar were set at Level -1.

The second set of validation experiments (V2) was devised to understand if the variables identified as being the most significant in the PB design ( $p < 0.10$ ) could trigger the accumulation of carotenoids in *P. gyrams* when cultured under the optimum growth conditions (Opt) for biomass production, as described in a previous work of our research group<sup>25</sup>. Briefly, Opt (Table 3) presents the optimal values for the growth factors: light intensity ( $x_3$ ), NaNO<sub>3</sub> ( $x_5$ ), NaH<sub>2</sub>PO<sub>4</sub> H<sub>2</sub>O ( $x_6$ ), and CuSO<sub>4</sub> 5H<sub>2</sub>O ( $x_{15}$ ). Regarding the non-significant independent variables identified in the PB matrix for biomass production, inoculum size ( $x_1$ ), airflow ( $x_4$ ), and NaHCO<sub>3</sub> concentration ( $x_{11}$ ) were set at Level -1, while the remaining growth parameters were set at Level 0. In addition to the assay Opt, that was used as control, this formulation was modified to promote the accumulation of all carotenoids (TCar), and fucoxanthin (Fx1ph and Fx2ph) Table 3.

x	Assay																											
	1	2	3	4	5	6	7	8	9	10	11	12	13	14	15	16	17	18	19	20	21	22	23	24	25	26	27	28
1	1	1	1	1	1	-1	1	-1	1	1	-1	-1	1	1	-1	-1	1	-1	1	-1	-1	-1	-1	-1	0	0	0	0
2	-1	1	1	1	1	1	-1	1	-1	1	1	-1	-1	1	1	-1	-1	1	-1	1	-1	-1	-1	-1	0	0	0	0
3	-1	-1	1	1	1	1	1	-1	1	-1	1	1	-1	-1	1	1	-1	-1	1	-1	1	-1	-1	-1	0	0	0	0
4	-1	-1	-1	1	1	1	1	1	-1	1	-1	1	1	-1	-1	1	1	-1	-1	1	-1	1	-1	-1	0	0	0	0
5	-1	-1	-1	-1	1	1	1	1	1	-1	1	-1	1	1	-1	-1	1	1	-1	-1	1	-1	1	-1	0	0	0	0
6	1	-1	-1	-1	-1	1	1	1	1	1	-1	1	-1	1	1	-1	-1	1	1	-1	-1	1	-1	-1	0	0	0	0
7	-1	1	-1	-1	-1	-1	1	1	1	1	1	-1	1	-1	1	1	-1	-1	1	1	-1	-1	1	-1	0	0	0	0
8	1	-1	1	-1	-1	-1	-1	1	1	1	1	1	-1	1	-1	1	1	-1	-1	1	1	-1	-1	-1	0	0	0	0
9	-1	1	-1	1	-1	-1	-1	-1	1	1	1	1	1	-1	1	-1	1	1	-1	-1	1	1	-1	-1	0	0	0	0
10	-1	-1	1	-1	1	-1	-1	-1	-1	1	1	1	1	1	-1	1	-1	1	1	-1	-1	1	1	-1	0	0	0	0
11	1	-1	-1	1	-1	1	-1	-1	-1	-1	1	1	1	1	1	-1	1	-1	1	1	-1	-1	1	-1	0	0	0	0
12	1	1	-1	-1	1	-1	1	-1	-1	-1	-1	1	1	1	1	1	-1	1	-1	1	1	-1	-1	-1	0	0	0	0
13	-1	1	1	-1	-1	1	-1	1	-1	-1	-1	-1	1	1	1	1	1	-1	1	-1	1	1	-1	-1	0	0	0	0
14	-1	-1	1	1	-1	-1	1	-1	1	-1	-1	-1	-1	1	1	1	1	1	-1	1	-1	1	1	-1	0	0	0	0
15	1	-1	-1	1	1	-1	-1	1	-1	1	-1	-1	-1	-1	1	1	1	1	1	-1	1	-1	1	-1	0	0	0	0
16	1	1	-1	-1	1	1	-1	-1	1	-1	1	-1	-1	-1	-1	1	1	1	1	1	1	-1	1	-1	0	0	0	0
17	-1	1	1	-1	-1	1	1	-1	-1	1	-1	1	-1	-1	-1	-1	1	1	1	1	1	-1	1	-1	0	0	0	0

**Table 2.** Coded values of each independent variable (x) used in the twenty-eight assays performed in the Plackett–Burman design.

	V1				V2			
	Con	Fx	$\beta$ Car	TCar	Opt	Fx1ph	Fx2ph	TCar
Inoculum size (AFDW g L <sup>-1</sup> )	0.1	0.1	0.1	0.1	0.1	0.1	0.1	0.1
Salinity (psu)	30	20	20	<b>20</b>	30	30	30	<b>20</b>
Light intensity	150	<b>150</b>	150	<b>150</b>	<u>700</u>	<b>150</b>	<b>700/150</b>	<b>150</b>
Air flow (mL min <sup>-1</sup> )	600	600	600	600	600	600	600	600
NaNO <sub>3</sub> (mg L <sup>-1</sup> )	100	<b>750</b>	<b>750</b>	<b>750</b>	<u>1500</u>	<b>1500</b>	<b>1500</b>	<b>1500</b>
NaH <sub>2</sub> PO <sub>4</sub> H <sub>2</sub> O (mg L <sup>-1</sup> )	20	10	10	10	<u>40</u>	<u>40</u>	<u>40</u>	<u>40</u>
Na <sub>2</sub> H <sub>2</sub> EDTA 2H <sub>2</sub> O (mg L <sup>-1</sup> )	45	22.5	22.5	22.5	45	45	45	45
H <sub>3</sub> BO <sub>3</sub> (mg L <sup>-1</sup> )	33.6	16.8	16.8	16.8	33.6	33.6	33.6	33.6
FeCl <sub>3</sub> 6H <sub>2</sub> O (mg L <sup>-1</sup> )	1.3	0.65	<b>1.95</b>	<b>1.95</b>	1.3	1.3	1.3	<b>1.95</b>
MnCl <sub>2</sub> 4H <sub>2</sub> O ( $\mu$ g L <sup>-1</sup> )	360	180	180	180	360	360	360	360
NaHCO <sub>3</sub> (mg L <sup>-1</sup> )	–	170	170	170	170	170	170	170
ZnCl <sub>2</sub> ( $\mu$ g L <sup>-1</sup> )	21	10.25	10.25	10.25	21	21	21	21
CoCl <sub>2</sub> 6H <sub>2</sub> O ( $\mu$ g L <sup>-1</sup> )	20	10	10	<b>30</b>	20	20	20	<b>30</b>
(NH <sub>4</sub> ) <sub>6</sub> Mo <sub>7</sub> O <sub>24</sub> 4H <sub>2</sub> O ( $\mu$ g L <sup>-1</sup> )	9	4.5	4.5	4.5	9	9	9	9
CuSO <sub>4</sub> 5H <sub>2</sub> O ( $\mu$ g L <sup>-1</sup> )	20	10	10	10	<u>6</u>	<u>6</u>	<u>6</u>	<u>6</u>
Thiamin ( $\mu$ g L <sup>-1</sup> )	100	50	50	50	100	100	100	100
Cyanocobalamin ( $\mu$ g L <sup>-1</sup> )	5	2.5	2.5	2.5	5	5	5	5

**Table 3.** Levels of the growth parameters used in the validation experiments. In V1, Walne's medium (control—Con) was compared to the maximized conditions for accumulation of fucoxanthin (Fx),  $\beta$ -carotene ( $\beta$ Car), and the sum of all carotenoids analyzed (TCar). The set V2 represents the maximized conditions for TCar and fucoxanthin accumulation using the optimized growth conditions for *P. gyra*ns' biomass production (Opt). Two strategies for fucoxanthin production were evaluated: 150  $\mu$ mol photons m<sup>-2</sup> s<sup>-1</sup> during the entire growth (Fx1ph) and a two-phase growth (Fx2ph) using 700  $\mu$ mol photons m<sup>-2</sup> s<sup>-1</sup> for the first 8 days and 150  $\mu$ mol photons m<sup>-2</sup> s<sup>-1</sup> for the last 2 days (stationary phase). Bold numbers represent the most significant variables and their values according to the calculated effects in Plackett–Burman. Underlined numbers represent the optimum growth conditions achieved for the maximal biomass production of *P. gyra*ns.

Regarding Fx, two different strategies were applied. In the assay Fx1ph, the whole growth of *P. gyra*ns was performed under the same light intensity (150  $\mu$ mol photons m<sup>-2</sup> s<sup>-1</sup>). On the other hand, and according to the light intensity used, the growth in the Fx2ph experiment was divided into two phases. First, *P. gyra*ns was grown at the optimal light intensity for biomass production (700  $\mu$ mol photons m<sup>-2</sup> s<sup>-1</sup>) until the end of the exponential growth phase; in the second phase, lasting 2 days, the light intensity was reduced to 150  $\mu$ mol photons m<sup>-2</sup> s<sup>-1</sup> to increase the Fx content of *P. gyra*ns. Since NaNO<sub>3</sub> showed a positive effect on Fx and TCar, and the concentration defined in the maximized growth conditions for biomass production was higher than those set in the PB design, the V2 experiments were supplemented with 1500 mg L<sup>-1</sup> of NaNO<sub>3</sub>. All experiments were performed in triplicate.

## Biomass characterization

### Pigment extraction, identification, and quantification by HPLC–DAD

Pigment analysis was conducted as described by Sanz et al.<sup>28</sup> with some modifications. Carotenoids were extracted from 10 mg of freeze-dried biomass in a screw cap glass tube with 3 mL of cold extraction solution (90% acetone, 0.1% BHT). Tubes were kept in ice and protected from light during all steps. Samples were left extracting for 15 min to allow acetone penetrating in microalgae structures, then they were vortexed for 30 s followed by 5 min in an ultrasonic bath. Extracts were centrifuged for 15 min at 358 g (Hettich Mikro 120, Tuttlingen, Germany) and the supernatant was collected. The pellet was re-extracted until it was colorless. From the total extract, 1 mL was syringe filtered (0.22  $\mu$ m nylon) to an amber vial, and received 0.3 mL of ultra-pure H<sub>2</sub>O to avoid incompatibility of solvents in the HPLC–DAD<sup>29</sup>.

The extracts were analyzed in a Shimadzu Nexera X2 system equipped with a 30AD liquid chromatograph, a SIL-30AC autosampler, a CTO-20AC column oven, a SPD-M20A diode array detector, and a CBM-20A Communication Bus Module. The pigments separation was performed through an ACE C18 PFP column 150 mm  $\times$  4.6 mm, 3  $\mu$ m particle size (Advanced Chromatography Technologies, Aberdeen, Scotland) at 40 °C. The mobile phase was a mixture of methanol:225 mM ammonium acetate (82:18, v:v) as eluent A and ethanol as eluent B. The gradient followed the indications of Sanz et al.<sup>28</sup> with some modifications: 96%:4% eluent A:eluent B (0–16 min), 62%:38% eluent A:eluent B (16–22 min), 62%:38% eluent A:eluent B (22–28 min), 28%:72% eluent A:eluent B (28–35 min), 20%:80% eluent A:eluent B (35–45 min), 20%:80% eluent A:eluent B (45–50 min) and 96%:4% eluent A:eluent B (50–55 min). The flow rate was 1 mL min<sup>-1</sup>, the run duration 55 min, and the injection volume 20  $\mu$ L. All reagents used in pigment extraction and chromatography analysis were HPLC grade. Identification of the extracted pigments was accomplished by comparison of the retention times and absorption spectra with commercial standards. Standards for chlorophyll *a*, chlorophyll *c*<sub>1</sub>, chlorophyll *c*<sub>2</sub>, fucoxanthin, all-*trans*- $\beta$ -carotene, diadinoxanthin, and diatoxanthin were obtained from DHI (Hørsholm, Denmark). The

identification of  $\alpha$ -carotene ( $\alpha$ Car) was done only by absorption spectra and retention time. All analysis were performed in triplicate.

#### Biomass and carotenoids productivity of *P. gyrans*

Volumetric productivity of the carotenoids ( $P_C$ ) and the biomass ( $P_X$ ) produced by *P. gyrans* was calculated using the following equations:

$$P_C (\text{mg L}^{-1} \text{ d}^{-1}) = \frac{C_i \times (X_{t_f} - X_{t_0})}{t_f}$$

$$P_X (\text{g L}^{-1} \text{ d}^{-1}) = \frac{X_{t_f} - X_0}{t_f}$$

where  $C_i$  is the carotenoid content,  $\text{mg g}^{-1}$ , and  $X$  is the ash-free dry weight,  $\text{g L}^{-1}$ , of the sampling time, days, at the end ( $t_f$ ) and the beginning ( $t_0$ ) of *P. gyrans* growth.

### Statistical analysis

The growth parameters defined in the PB design as the most significant in the carotenoids production of *P. gyrans* were identified using a 90% confidence level ( $p < 0.10$ ), in order to avoid excluding any important independent variable<sup>27</sup>. The statistical analysis was performed with the online software Protimiza Experimental Design (<http://experimental-design.protimiza.com.br/>). The validation tests were evaluated for differences between means using one-way ANOVA followed by Tukey's multiple comparison test at 95% confidence level (GraphPad Prism version 8.0.2).

## Results and discussion

### Plackett–Burman design

Regarding the pigments composition of *P. gyrans*, the chromatogram achieved during the preliminary tests (see supplementary material), overall, allowed to confirm the pigment profile commonly described for this species and other Pavlovophyceae species<sup>21,30</sup>. Eight pigments were identified: three chlorophylls and five carotenoids. Despite the identification of chlorophylls  $a$ ,  $c_1$  and  $c_2$ , they were not quantified because the goal of this work was to study the ability of *P. gyrans* to accumulate carotenoid pigments, reason why statistics and discussion are focused on carotenoids. Among the carotenoids, it was possible to identify fucoxanthin (Fx), diadinoxanthin (Ddx), diatoxanthin (Dtx),  $\beta$ -carotene ( $\beta$ Car) and  $\alpha$ -carotene ( $\alpha$ Car), which match to the carotenoid composition described in other strains of *P. gyrans*<sup>30</sup>.

According to their role on microalgae, these pigments can be classified as primary pigments—if they are part of the light-harvesting complexes (LHCs), located in thylakoid membranes, and are involved in light capture and photosynthetic activity<sup>31</sup>—or secondary pigments—those with a photoprotective role and which production is triggered under stressful growth conditions. Among the pigments present in *P. gyrans*, chlorophylls  $a$ ,  $c_1$ , and  $c_2$ , as well as Fx, are part of the LHCs, while Ddx, Dtx, and  $\beta$ Car act as a photoprotective agents<sup>32</sup>.

The influence of the twenty-eight growth parameters combinations tested on the carotenoids' composition of *P. gyrans* is present in Table 4. Fx content ranged from 3.409  $\text{mg g}^{-1}$  DW in assay #13 to 0.401  $\text{mg g}^{-1}$  DW in assay #3. The extreme values for Ddx were obtained in the assays #13 and #3 with 1.068 and 0.113  $\text{mg g}^{-1}$  DW, respectively, whereas the Dtx content varied from 0.091 (#4) to 1.678  $\text{mg g}^{-1}$  DW (#17). Regarding the carotene production, the highest values of  $\beta$ Car and  $\alpha$ Car were 0.491 (#11) and 0.545  $\text{mg g}^{-1}$  DW (#9) while the lowest were 0.151 (#27) and 0.114  $\text{mg g}^{-1}$  DW (#18). Finally, and summing all the carotenoids previously mentioned, the total carotenoids content ranged from 6.743 (#13) to 1.017  $\text{mg g}^{-1}$  DW (#4). The wide variation achieved for each carotenoid, as well as its total content, represents well the key role of the growth conditions and nutrient availability in microalgae metabolism, which in this case had as main outcome a diversified carotenoids' composition.

Data from Table 4 were used to calculate the effect of each independent variable (growth parameter) on the accumulation of each carotenoid (dependent variable), using a statistical significance lower than 10% to identify the most significant independent factors (Table 5). Fx production by *P. gyrans* was promoted by decreasing light intensity ( $p < 0.001$ ) and increasing  $\text{NaNO}_3$  ( $p = 0.006$ ), which means that these variables had a negative and positive effect on this carotenoid, respectively. These variables also had a similar impact on Ddx content, together with salinity, whose lower values increased the accumulation of Ddx ( $p = 0.031$ ).

Results showed that  $\beta$ Car was positively correlated with higher supplementation of  $\text{NaNO}_3$  ( $p = 0.046$ ) and  $\text{FeCl}_3 \cdot 6\text{H}_2\text{O}$  ( $p = 0.062$ ), whereas for  $\alpha$ Car none of the independent variables was statistically significant within the tested ranges ( $p > 0.10$ ). Dtx was identified as the carotenoid with the highest number of significant variables (7). Concerning the sum of all carotenoids of *P. gyrans*, three abiotic factors with statistical importance were identified: light intensity ( $p < 0.001$ ),  $\text{NaNO}_3$  ( $p = 0.001$ ), and  $\text{FeCl}_3 \cdot 6\text{H}_2\text{O}$  ( $p = 0.038$ ). As already mentioned for individual carotenoids, nitrogen and copper concentrations in the medium were positively correlated with total carotenoids content, in contrast to the light intensity. In order to avoid excluding any important variable, the nutrient  $\text{CoCl}_2 \cdot 6\text{H}_2\text{O}$  and the salinity level of the medium were also considered significant variables, given the closeness of their  $p$ -values ( $p = 0.103$ – $0.104$ ) to the statistical significance threshold adopted. Among the dependent variables assessed, only Fx, Dtx, and TCar presented a significant curvature ( $p < 0.10$ ), meaning that the optimal value for these carotenoids was reached within the range of abiotic factors tested. Overall, the abiotic factors here identified with a marked effect on the carotenoid composition of *P. gyrans* are in accordance with described in literature, and their effects are discussed below.

#Assay	Fucoxanthin (mg g <sup>-1</sup> DW)	Diatoxanthin (mg g <sup>-1</sup> DW)	Diadinoxanthin (mg g <sup>-1</sup> DW)	β-carotene (mg g <sup>-1</sup> DW)	α-carotene (mg g <sup>-1</sup> DW)	Total carotenoids (mg g <sup>-1</sup> DW)
1	1.670 ± 0.047	0.707 ± 0.014	0.427 ± 0.005	0.342 ± 0.005	0.413 ± 0.008	3.587 ± 0.052
2	1.942 ± 0.008	0.620 ± 0.002	0.341 ± 0.003	0.257 ± 0.002	0.265 ± 0.002	3.426 ± 0.018
3	0.401 ± 0.002	0.093 ± 0.000	0.113 ± 0.000	0.277 ± 0.001	0.242 ± 0.060	1.127 ± 0.003
4	0.444 ± 0.000	0.091 ± 0.000	0.113 ± 0.000	0.231 ± 0.002	0.137 ± 0.002	1.017 ± 0.004
5	0.933 ± 0.007	0.183 ± 0.002	0.184 ± 0.001	0.387 ± 0.001	0.421 ± 0.001	2.107 ± 0.011
6	1.417 ± 0.024	0.190 ± 0.001	0.282 ± 0.014	0.285 ± 0.015	0.342 ± 0.019	2.517 ± 0.023
7	0.570 ± 0.008	0.200 ± 0.001	0.194 ± 0.001	0.278 ± 0.013	0.193 ± 0.008	1.437 ± 0.023
8	2.161 ± 0.017	0.334 ± 0.003	0.554 ± 0.007	0.174 ± 0.009	0.245 ± 0.011	3.468 ± 0.045
9	0.765 ± 0.002	0.257 ± 0.001	0.410 ± 0.003	0.482 ± 0.003	0.545 ± 0.004	2.460 ± 0.013
10	1.118 ± 0.011	0.331 ± 0.006	0.207 ± 0.006	0.289 ± 0.007	0.338 ± 0.008	2.282 ± 0.035
11	0.846 ± 0.013	0.184 ± 0.003	0.167 ± 0.051	0.491 ± 0.009	0.461 ± 0.005	2.149 ± 0.027
12	0.482 ± 0.002	0.323 ± 0.001	0.247 ± 0.001	0.225 ± 0.008	0.194 ± 0.008	1.471 ± 0.016
13	3.409 ± 0.068	1.474 ± 0.017	1.068 ± 0.005	0.396 ± 0.002	0.395 ± 0.003	6.743 ± 0.078
14	1.896 ± 0.035	0.798 ± 0.009	0.393 ± 0.015	0.210 ± 0.007	0.221 ± 0.008	3.518 ± 0.022
15	0.469 ± 0.004	0.258 ± 0.003	0.183 ± 0.001	0.244 ± 0.004	0.230 ± 0.004	1.385 ± 0.014
16	0.421 ± 0.10	0.415 ± 0.011	0.237 ± 0.007	0.191 ± 0.002	0.191 ± 0.002	1.454 ± 0.023
17	3.290 ± 0.015	1.678 ± 0.008	0.991 ± 0.007	0.312 ± 0.003	0.286 ± 0.003	6.557 ± 0.036
18	3.351 ± 0.024	0.476 ± 0.003	0.767 ± 0.005	0.206 ± 0.003	0.114 ± 0.001	4.915 ± 0.036
19	0.467 ± 0.033	0.134 ± 0.010	0.154 ± 0.009	0.250 ± 0.020	0.173 ± 0.014	1.178 ± 0.086
20	1.850 ± 0.024	0.488 ± 0.007	0.375 ± 0.006	0.195 ± 0.005	0.213 ± 0.007	3.121 ± 0.044
21	0.799 ± 0.006	0.242 ± 0.002	0.322 ± 0.002	0.463 ± 0.004	0.642 ± 0.005	2.468 ± 0.013
22	1.651 ± 0.167	0.401 ± 0.049	0.600 ± 0.074	0.285 ± 0.046	0.352 ± 0.056	3.290 ± 0.363
23	1.599 ± 0.213	0.836 ± 0.127	0.526 ± 0.072	0.233 ± 0.041	0.322 ± 0.048	3.515 ± 0.499
24	1.656 ± 0.005	0.375 ± 0.001	0.526 ± 0.002	0.189 ± 0.002	0.228 ± 0.002	2.975 ± 0.007
25	0.837 ± 0.020	0.122 ± 0.002	0.443 ± 0.004	0.292 ± 0.001	0.332 ± 0.010	2.025 ± 0.025
26	0.762 ± 0.004	0.218 ± 0.001	0.326 ± 0.001	0.180 ± 0.012	0.207 ± 0.014	1.693 ± 0.019
27	0.695 ± 0.011	0.237 ± 0.004	0.278 ± 0.004	0.151 ± 0.008	0.182 ± 0.006	1.543 ± 0.032
28	0.957 ± 0.073	0.186 ± 0.016	0.182 ± 0.014	0.324 ± 0.045	0.387 ± 0.052	2.037 ± 0.200

**Table 4.** Carotenoids composition, mg g<sup>-1</sup>, of *P. gyrans* produced in the Plackett–Burman design.

	Fucoxanthin (mg g <sup>-1</sup> )		Diatoxanthin (mg g <sup>-1</sup> )		Diadinoxanthin (mg g <sup>-1</sup> )		β-carotene (mg g <sup>-1</sup> )		α-carotene (mg g <sup>-1</sup> )		Total Carotenoids (mg g <sup>-1</sup> )	
	Effect	<i>p</i> -value	Effect	<i>p</i> -value	Effect	<i>p</i> -value	Effect	<i>p</i> -value	Effect	<i>p</i> -value	Effect	<i>p</i> -value
Mean	1.402	<b>0.000</b>	0.462	<b>0.000</b>	0.391	<b>0.000</b>	0.287	<b>0.000</b>	0.299	<b>0.000</b>	2.840	<b>0.000</b>
Curvature	- 1.177	<b>0.052</b>	- 0.543	<b>0.020</b>	- 0.167	0.365	- 0.101	0.291	- 0.043	0.784	- 2.032	<b>0.023</b>
Inoculum size	0.020	0.923	0.170	<b>0.043</b>	- 0.016	0.816	0.044	0.226	0.008	0.894	0.226	0.441
Salinity	0.002	0.993	- 0.250	<b>0.007</b>	- 0.169	<b>0.031</b>	- 0.033	0.352	- 0.059	0.335	- 0.509	<b>0.103</b>
Light intensity	- 1.467	<b>0.000</b>	- 0.496	<b>0.000</b>	- 0.347	<b>0.001</b>	0.060	0.113	0.032	0.598	- 2.219	<b>0.000</b>
Air flow	0.155	0.457	0.094	0.227	0.060	0.387	- 0.033	0.357	- 0.046	0.450	0.230	0.433
NaNO <sub>3</sub>	0.703	<b>0.006</b>	0.218	<b>0.015</b>	0.195	<b>0.017</b>	0.079	<b>0.046</b>	0.101	0.114	1.295	<b>0.001</b>
NaH <sub>2</sub> PO <sub>4</sub> H <sub>2</sub> O	- 0.128	0.534	- 0.189	<b>0.028</b>	- 0.045	0.511	- 0.029	0.410	- 0.037	0.538	- 0.429	0.160
Na <sub>2</sub> H <sub>2</sub> EDTA 2H <sub>2</sub> O	- 0.200	0.341	- 0.002	0.977	- 0.046	0.508	0.006	0.871	- 0.002	0.974	- 0.244	0.406
H <sub>3</sub> BO <sub>3</sub>	- 0.182	0.385	0.051	0.501	- 0.041	0.550	0.034	0.341	0.068	0.267	- 0.070	0.808
FeCl <sub>3</sub> 6H <sub>2</sub> O	0.291	0.177	0.132	0.102	0.121	0.101	0.072	<b>0.062</b>	0.063	0.304	0.680	<b>0.038</b>
MnCl <sub>2</sub> 4H <sub>2</sub> O	- 0.041	0.842	0.017	0.816	- 0.005	0.945	- 0.001	0.977	- 0.026	0.658	- 0.056	0.846
NaHCO <sub>3</sub>	0.175	0.402	0.269	<b>0.005</b>	0.039	0.569	- 0.005	0.879	- 0.032	0.590	0.446	0.146
ZnCl <sub>2</sub>	0.167	0.422	0.107	0.175	0.008	0.908	- 0.009	0.804	- 0.015	0.800	0.258	0.381
CoCl <sub>2</sub> 6H <sub>2</sub> O	0.251	0.239	0.182	<b>0.033</b>	0.091	0.202	- 0.017	0.629	0.001	0.992	0.508	<b>0.104</b>
(NH <sub>4</sub> ) <sub>6</sub> Mo <sub>7</sub> O <sub>24</sub> 4H <sub>2</sub> O	- 0.019	0.927	0.075	0.330	0.035	0.607	- 0.050	0.173	- 0.089	0.156	- 0.048	0.868
CuSO <sub>4</sub> 5H <sub>2</sub> O	- 0.011	0.956	0.023	0.753	- 0.004	0.949	- 0.021	0.558	- 0.012	0.845	- 0.025	0.931
Thiamin	0.302	0.163	0.031	0.674	0.041	0.553	0.039	0.275	0.033	0.586	0.446	0.146
Cyanocobalamin	0.078	0.703	0.011	0.883	- 0.029	0.675	- 0.029	0.410	- 0.043	0.478	- 0.012	0.967

**Table 5.** Calculated effects for each carotenoid of *P. gyrans* from the Plackett–Burman experimental design. Bold numbers represent the abiotic factors with *p*-values considered statistically significant (*p* < 0.10).

### Light intensity

Light plays a crucial role in photosynthetic organisms, providing the energy needed for the carbon fixation that will be metabolized for further biocompounds synthesis and cell growth. Similarly to the results here reported for *P. gyrans*, increasing light intensity in nitrogen-stressed cells of *D. lutheri* contributed to a sharp decrease (> 50%) in total carotenoids content<sup>32</sup>. These authors argued that, at higher light intensities, the N-starvation condition triggered the accumulation of Ddx and Dtx, mainly at the expense of  $\beta$ Car. Similarly, *P. gyrans* grown under three different illumination levels achieved the lowest fucoxanthin/chlorophyll *a* ratio and greater growth rates with increasing light intensity. Higher light intensity led to an overall decrease in pigment content, both in photosynthetic and photoprotective pigments<sup>33</sup>. As reported for the haptophyte *Emiliania huxleyi*, the photoacclimation process has as the main goal to optimize photosynthesis efficiency by changing the composition of the LHC. At low light intensity, this is reached by increasing the amounts of photosynthetic pigments and proteins LHCF<sup>34</sup>. LHC of *P. gyrans* is composed by a Fx-Chl *a/c*-protein complex<sup>31</sup>, which explains the negative effect of the light intensity over the pigments composition here reported.

### Nitrogen

Regarding the NaNO<sub>3</sub>, a comparable trend was described for the Fx content of *Pavlova* OPMS 30,543, whose value increased in culture medium supplemented with higher levels of nitrate<sup>35</sup>. Such trend was also stated in other microalgae genus like *Phaeodactylum*<sup>36</sup> and *Odontella*<sup>37</sup>. Likewise, the total carotenoids content of *P. pinguis* had a substantial increase (58 times) when the nitrogen supplementation changed from 140 to 1752  $\mu\text{mol L}^{-1}$  NaNO<sub>3</sub><sup>38</sup>. Longworth et al.<sup>39</sup> verified that nitrogen-stressed *P. tricornutum* cells showed a significant reduction in the photosynthetic pathway due to the lower abundance of enzymes responsible for carbon fixation, as well less presence of proteins and pigments in the photosynthetic apparatus. The reason for that relies on its chemical composition, which possesses a high content of nitrogen. Therefore, to maximize the nitrogen availability for protein synthesis indispensable for cell subsistence, stressed cells down-regulate the photosynthetic pathway, causing a decrease in their pigments<sup>39</sup>.

### Salinity

Under salinity stress, microalgae tend to increase the intracellular composition of the signaling molecules, such as calcium and reactive oxygen species (ROS)<sup>40</sup>. By reacting with macromolecules (e.g., DNA, proteins), ROS can severely impair the cell metabolism or even lead to death. In order to counteract ROS action, cell activates anti-oxidant defense mechanisms, which may involve increased production of antioxidant compounds<sup>40,41</sup>. Overall, salinity stress has been especially highlighted as a key factor responsible for causing the accumulation of carotenoids in several microalgae from the genus *Dunaliella*<sup>42</sup>, *Chlorella*<sup>43</sup>, *Desmodemus*<sup>44</sup>, and *Haematococcus*<sup>40</sup>. For instance, *Dunaliella tertiolecta* grown under extreme salinities (3 M) was shown to have a marked increase—at cellular basis—of  $\beta$ Car, although the negative impact in the microalgae growth performance<sup>42</sup>. *Desmodemus* sp. also presented a total carotenoid content 2.7-fold higher when subjected to salt stress conditions<sup>44</sup>.

However, the TCar of *P. gyrans* (Table 5) had a negative impact promoted by salinity. Despite the different salinity range tested, the Fx content of marine species *Tisochrysis lutea* and *P. tricornutum* also presented a significant drop when grown with increasing salinities beyond the optimal level (35–45 ‰)<sup>45</sup>. The authors also discussed that, although the suboptimal salinity levels tested led to stressful conditions for the photosynthetic apparatus of the cells, the impact on photosynthetic pigment production (e.g., fucoxanthin) remains unclear. This particular evidence points out the species-dependent behavior of each microalga for the same abiotic factor.

### Iron

Iron is an important micronutrient for several cellular processes, such as DNA synthesis, respiration, and photosynthesis. It is a crucial cofactor for enzymatically mediated processes, which allow the physiological and chemical balance, as well as a key nutrient for chlorophyll synthesis and chloroplasts stability<sup>46</sup>, and the anti-oxidant mechanism against ROS<sup>47</sup>. In fact, Fe limitation has been described as a limiting nutrient in oceanic waters, even those with higher concentrations of macronutrients (i.e. N and P)<sup>48</sup>. In this work, the increasing concentrations of iron within the range tested showed a positive effect on carotenoids accumulation of *P. gyrans*. Fe is a key component in the nitrogen assimilation, a nutrient itself that develops a crucial role in the photosynthetic pathways, as previously explained in the “Nitrogen” section. The overall increase of carotenoids at higher Fe supplementation may be explained by its high concentration in the chloroplasts and, especially, in the photosystem I (PSI)—12 Fe per PSI<sup>47</sup>. PSI and PSII are pigment-protein complexes which may contain different pigments, namely chlorophyll *a*, *c*<sub>1</sub> + *c*<sub>2</sub>, beta-carotene, and xanthophylls, being the Fe availability strictly connected to the pigment modulation of the PS<sup>49</sup>. The deficient supply of iron in *Chlamydomonas reinhardtii* induced the remodeling of LHCI, by processing and up- or down regulation of its pigment-binding proteins, with a concomitant decrease of excitation energy efficiency to the PSI<sup>47</sup>. Kosakowska et al.<sup>48</sup> reported a similar trend in *P. tricornutum*, whose cells were grown in a range of 0.001 to 10  $\mu\text{mol L}^{-1}$  Fe<sup>3+</sup>, with higher concentrations promoting the highest contents of chlorophyll *a*, *c*<sub>1</sub> + *c*<sub>2</sub>, Fx, Ddx, and  $\beta$ carotene. The authors also noticed that the iron-deficient cells presented a marked decrease of its  $\beta$ Car, a conclusion that is in line with *P. gyrans* considering the relevance ( $p = 0.062$ ) achieved for FeCl<sub>3</sub>·6H<sub>2</sub>O (Table 5).

### Cobalt

Cobalt is an important micronutrient for microalgae, mainly due to its role as structural molecule involved in the synthesis of the important cofactor cobalamin, which in turn influences the enzymatic processes responsible for nitrogen fixation<sup>50</sup>. However, when supplied at higher concentrations, this heavy metal can be harmful for microalgae as consequence of the increasing oxidative stress<sup>51</sup>, a phenomenon always described as species-dependent.

In the present work, cobalt had a positive impact on TCar, Dtx, and  $\alpha$ Car content of *P. gyrans*. Indeed, the increasing accumulation of protective carotenoids (e.g., Dtx) under higher cobalt concentrations might be seen as the response of *P. gyrans* against the likely production of ROS during electron acceptor–donor interactions of cobalt<sup>52</sup>. The supplementation of cobalt at low levels proved to be successful for microalgae growth and carotenogenesis in *Spirulina platensis*<sup>53</sup>, *Monoraphidium minutum*, and *Nitzschia perminuta*<sup>54</sup>. Although the decreasing content in both classes of pigments, the authors also highlighted the superior stability of carotenoids at higher cobalt levels, in contrast to chlorophyll<sup>54</sup>.

For practical reasons, only three responses (those allowing to maximise Fx,  $\beta$ Car, and TCar) were considered in the validation assays. The aim was to confirm the potential of *P. gyrans* as a carotenoid producer, in particular of the commercially important and demanded  $\beta$ Car and, mostly, Fx. Considering the interconnected and dependent production of Dtx and Ddx (xanthophyll cycle), the individual validation of these carotenoids was passed over in favor of TCar.

## Validation tests

### Growth analysis

The culture conditions applied in the validation assays are presented in Table 3. The growth performance of *P. gyrans* under the validation conditions of set V1 is presented in Fig. 1. Despite the decreasing concentration in ten nutrients, *P. gyrans* grown in the assay Fx,  $\beta$ Car, and TCar had longer growth and higher  $X_{max}$  values when compared to the control medium (Con) (see Supplementary Table S1). Among the same seventeen growth parameters, nitrogen supplementation, along with light intensity and copper, were identified in a previous work of our research group as the most important factors in biomass production of *P. gyrans*<sup>25</sup>. As the Fx,  $\beta$ Car, and TCar maximization assays share the same levels of  $\text{NaNO}_3$  (7.5 times higher than Con) and copper (2 times lower than Con), the  $\approx$ twofold increase in final  $X_{max}$  and  $P_x$  may be explained by the variation in these growth conditions.

Regarding the validation set V2, it was verified that *P. gyrans* grown in the assay Opt.V2 and Fx2ph.V2 showed significantly higher  $X_{max}$  and  $P_x$  compared to the experiments Fx1ph.V2 and TCar.V2 (see Supplementary Table S1). The improved biomass production in Opt.V2 and Fx2ph.V2 may be related to the higher illumination, which was used during the whole growth and until the end of the exponential growth phase, respectively. In

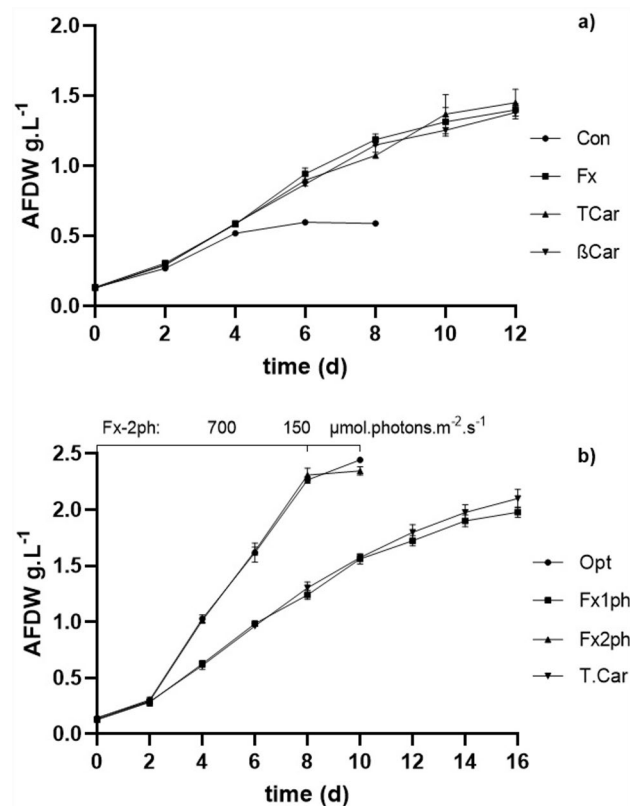


**Figure 1.** Growth profile of *P. gyrans* cultivated with the modified medium for the validation experiments V1 (a): Walne's medium (Con) and the maximized conditions for accumulation of fucoxanthin (Fx),  $\beta$ -carotene ( $\beta$ Car), and the sum of all carotenoids analyzed (TCar). In V2 (b) was assessed the optimized growth conditions for *P. gyrans*' biomass production (Opt) and the maximized growth conditions for TCar and fucoxanthin: 150  $\mu\text{mol photons m}^{-2} \text{s}^{-1}$  during the entire growth (Fx1ph) or using 700  $\mu\text{mol photons m}^{-2} \text{s}^{-1}$  for the first 8 days and 150  $\mu\text{mol photons m}^{-2} \text{s}^{-1}$  for the last 2 days (Fx2ph). The experiments were performed in triplicate and the error bars represent the mean values and standard deviation.



fact, light intensity stood out as the most significant variable in our previous work aimed at optimizing biomass production of *P. gyrans*<sup>25</sup>, in which its optimal value was defined as 700  $\mu\text{mol photons m}^{-2} \text{s}^{-1}$ , the same used in Opt.V2 and Fx2ph.V2. The increase of light intensity from 150 to 700  $\mu\text{mol photons m}^{-2} \text{s}^{-1}$  was responsible for shortening by 6 days the growth of *P. gyrans*, which almost doubled its volumetric productivity (see Supplementary Table S1). Several works have described the increase in the growth performance with light intensity<sup>33,55</sup>.

#### Carotenoids composition

Carotenoids composition of *P. gyrans* produced in the validation experiments is described in Fig. 2.

Although the growth conditions tested were primarily aimed at maximizing Fx,  $\beta\text{Car}$ , and TCar content, the results obtained for Dtx, Ddx, and  $\alpha\text{Car}$  were also presented in all experiments. Regarding the Fx content, in validation set V1 it was seen that Con.V1 produced 2.010  $\text{mg g}^{-1} \text{DW}$ , nearly half of the concentration achieved in the remaining experiments (Fx.V1, TCar.V1, and  $\beta\text{Car.V1}$ ). The Fx values between Fx.V1, TCar.V1, and  $\beta\text{Car.V1}$  were similar ( $p > 0.05$ ), which can be justified by using the same level of the most significant variables for this carotenoid (light intensity and  $\text{NaNO}_3$ ). Similarly, in validation set V2, the control experiment (Opt) presented the lowest level of Fx, with 2.154  $\text{mg g}^{-1} \text{DW}$  ( $p < 0.05$ ). The two approaches carried out to improve Fx accumulation in *P. gyrans* were succeeded, with Fx2ph.V2 and Fx1ph.V2 reaching 3.294 and 4.879  $\text{mg g}^{-1} \text{DW}$ , respectively. Although the Fx content produced was lower than that achieved in the assays performed strictly at low light intensity, the approach tested on Fx2ph.V2 promoted a 1.5-fold increase in Fx concentration compared to Opt, without compromising biomass production (Fig. 1 and Supplementary Table S1). In opposition to V1, *P. gyrans* grown under TCar.V2 conditions promoted the highest Fx content ( $p < 0.05$ ), whose value reached 6.153  $\text{mg g}^{-1} \text{DW}$ . Such increase might be explained by a richer nutrient composition in V2, among which the notable increase in the  $\text{NaNO}_3$  level (1500 vs 750  $\text{mg L}^{-1}$ ) stands out.

Ddx presented a similar trend to that of Fx. In V1 set, all the conditions tested yielded higher Ddx contents than the control conditions ( $p < 0.05$ ), which values ranged from 1.273 to 3.368  $\text{mg g}^{-1} \text{DW}$ . In the V2 set, Opt showed, once again, the lowest content of Ddx (1.938  $\text{mg g}^{-1} \text{DW}$ ), with a significant increase in the accumulation of this carotenoid occurring as light intensity decreased, reaching its maximum in TCar.V2 (4.573  $\text{mg g}^{-1} \text{DW}$ ). With respect to Dtx, the conditions tested in V1 showed no significant differences, with the highest content produced by *P. gyrans* found in Fx.V1 (1.448  $\text{mg g}^{-1} \text{DW}$ ) and the lowest achieved in  $\beta\text{Car}$  (0.758  $\text{mg g}^{-1} \text{DW}$ ). Dtx profile had the opposite trend of the Ddx in V2 set. Dtx values ranged from 0.139 to 0.763  $\text{mg g}^{-1} \text{DW}$ , with the highest value being reached under high illumination (Opt.V2) and considered significantly higher than the remaining assays ( $p < 0.05$ ). The relationship between these xanthophylls is a well-known process (diadinoxanthin cycle) widely described in several haptophytes and diatoms, that is triggered against the oxidative stress promoted by high light conditions. Through enzyme-mediated processes, microalgae produce Dtx by de-epoxidation of Ddx at high irradiances; conversely, epoxidation of Dtx to Ddx occurs at low light intensities<sup>52</sup>. Due to its higher number of the conjugated double bonds<sup>56</sup>, Dtx proved increased performance in scavenging of free radicals and quenching of chlorophyll triple states, protecting and stabilizing the thylakoid membranes under high irradiances and temperatures<sup>8,52</sup>.

Among the carotenoids optimized,  $\beta\text{Car}$  had the lowest content. There were no significant differences between Con.V1, TCar.V1, and the theoretical optimal conditions ( $\beta\text{Car.V1}$ ) with their contents ranging between 0.455 and 0.629  $\text{mg g}^{-1} \text{DW}$ . Fx.V1 produced the lowest value of  $\beta\text{Car}$  ( $p < 0.05$ ). Considering that  $\text{FeCl}_3 \cdot 6\text{H}_2\text{O}$  was identified in the PB design as a key factor for the production of  $\beta\text{Car}$  by *P. gyrans*, its concentration may explain the low content of this carotenoid in Fx.V1. As displayed in Table 3, this assay was the only one that showed limited iron concentrations, thus validating the importance of the statistical approach conducted in this work. This observation is also corroborated by the results of V2. Although *P. gyrans* was not tested with culture conditions to increase the accumulation of  $\beta\text{Car}$ , like the  $\beta\text{Car.V1}$ , the only assay with a significant increase in this carotenoid was TCar.V2 (0.596  $\text{mg g}^{-1} \text{DW}$ ), which was also the only assay with a higher iron supplementation (1.95  $\text{mg L}^{-1}$ ). Regarding the  $\alpha\text{Car}$ , its value ranged between 0.540–0.843 and 0.322–0.524  $\text{mg g}^{-1} \text{DW}$  in the V1 and V2 experiments, respectively.

Considering that the most prominent carotenoids in *P. gyrans* were Fx and Ddx, these carotenoids strongly influenced the TCar content. In fact, TCar content among the assays matched the profile already described for Fx and Ddx. In the set V1, Con produced the lowest content ( $p < 0.05$ ) of total carotenoids, 5.633  $\text{mg g}^{-1} \text{DW}$ , whereas in Fx.V1, TCar.V1, and  $\beta\text{Car.V1}$  the range was 9.070–9.820  $\text{mg g}^{-1} \text{DW}$ . On the other hand, all the experiments of the set V2 presented significant differences among them ( $p < 0.05$ ). Considering the carotenoids content, whose value ranged from 5.614 to 11.794  $\text{mg g}^{-1} \text{DW}$ , the validation experiments can be ranked as TCar.V2 > Fx1ph.V2 > Fx2ph.V2 > Opt.V2. Indeed, the results reported here for TCar validate the findings produced with the statistical approach adopted. In both V1 and V2, the manipulation of the main abiotic factors according to PB (salinity, light intensity,  $\text{NaNO}_3$ ,  $\text{FeCl}_3 \cdot 6\text{H}_2\text{O}$ , and  $\text{CoCl}_2 \cdot 6\text{H}_2\text{O}$ ) proved successful, allowing a 1.7- and 2.1-fold increase in the final composition of *P. gyrans*, respectively.

Taking into consideration the assay with the highest yield in carotenoids (TCar.V2), the statistical approach here adopted led to a modified medium with improved production of Fx (6.153  $\text{mg g}^{-1} \text{DW}$ ) and TCar (11.794  $\text{mg g}^{-1} \text{DW}$ ). *P. gyrans* grown under those conditions showed a higher content of carotenoids compared to *D. lutheri* (5–6  $\text{mg g}^{-1} \text{AFDW}$ )<sup>32</sup> and *P. pinguis* (4.32–2.91  $\text{mg g}^{-1} \text{DW}$ )<sup>38,57</sup>. On the other hand, the Fx content of *Pavlova* sp. OPMS 30,543, grown under optimized growth conditions, reached 12.88  $\text{mg g}^{-1} \text{DW}$  at lab-scale, which rose to 20.86  $\text{mg g}^{-1} \text{DW}$  when grown at outdoor conditions<sup>35</sup>. Beyond the Pavlovophyceae, other species are well-known producers of carotenoids, especially Fx. Depending on the cultivation features, the Fx content described for the haptophyte *Tisochrysis lutea* was 5.51–10.73  $\text{mg g}^{-1}$ <sup>58</sup>. *Phaeodactylum tricorutum*<sup>36</sup> and *Odontella aurita*<sup>37</sup> were also highlighted as highly productive species, whose Fx content achieved was 42.8, 18.47, 18.18  $\text{mg g}^{-1}$ , respectively.

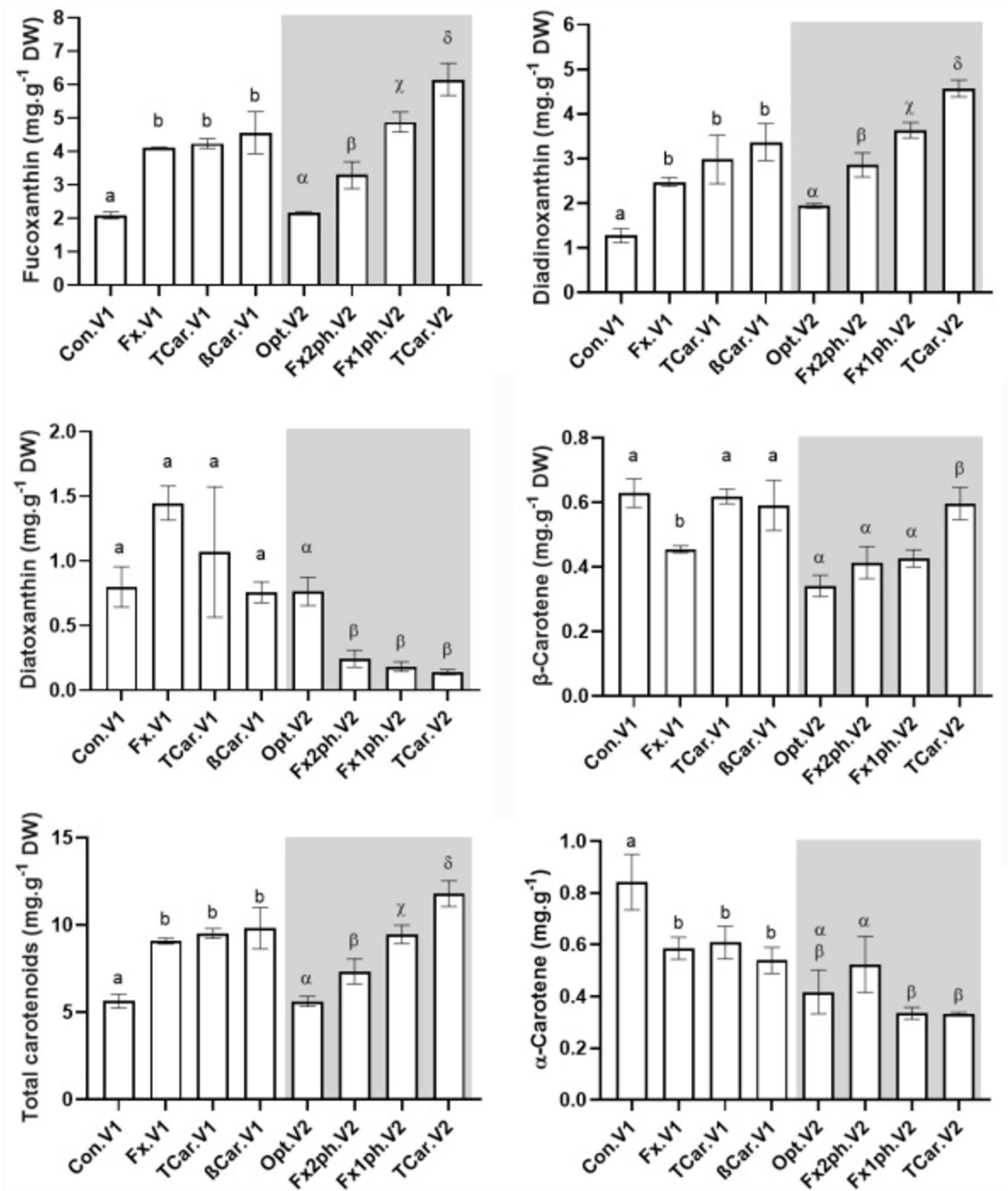


**Figure 2.** Carotenoids composition, mg g<sup>-1</sup>, of *P. gyrams* cultured in validation experiments (V1 and V2). In V1, was evaluated the Walne’s medium (Con) and the maximized conditions for accumulation of fucoxanthin (Fx), β-carotene (βCar), and the sum of all carotenoids analyzed (TCar). In V2 (b) was assessed the optimized growth conditions for *P. gyrams*’ biomass production (Opt) and the maximized growth conditions for TCar and fucoxanthin: 150 μmol photons m<sup>-2</sup> s<sup>-1</sup> during the entire growth (Fx1ph) or using 700 μmol photons m<sup>-2</sup> s<sup>-1</sup> for the first 8 days and 150 μmol photons m<sup>-2</sup> s<sup>-1</sup> for the last 2 days (Fx2ph). The assays were performed in triplicate, with the bars representing the mean values and the standard deviation. Bars over the grey background represent the values produced by the validation test 2 (V2). Means with different letters within each data set (V1 or V2) are significantly different (p < 0.05).

### Carotenoids productivity

The data from growth performance (Fig. 1) and the respective carotenoids content (Fig. 2) were used to calculate carotenoids productivity ( $\text{mg L}^{-1} \text{d}^{-1}$ ) of *P. gyrams* in the validation experiments (Fig. 3). In general, the values obtained for Con.V1 are in line with the previously described in “Carotenoids composition” section. The low biomass production, together with the low content of carotenoids—especially Fx, Ddx, and TCar—made the respective productivity values significantly lower than in the other assays (Fig. 3a). Furthermore, the different values of  $\beta$ Car productivity compared between Con.V1 and  $\beta$ Car.V1 should be pointed out. Although  $\beta$ Car.V1 showed a 4-day increase in growth duration, as well as lower  $\beta$ Car content, this assay achieved higher productivity than Con.V1. This improvement was due to the higher  $X_{max}$  achieved, which almost doubled in comparison with Con.V1 (see Supplementary Table S1). Thus, although  $\beta$ Car.V1 failed to increase  $\beta$ Car content (Fig. 2), these growth conditions proved advantageous for enhancing its productivity.

In the set V2, it was found that TCar.V2 and Fx2ph.V2 stood out as the most productive conditions for Fx ( $0.726\text{--}0.759 \text{ mg L}^{-1} \text{d}^{-1}$ ), Ddx ( $0.564\text{--}0.629 \text{ mg L}^{-1} \text{d}^{-1}$ ), and TCar ( $1.454\text{--}1.615 \text{ mg L}^{-1} \text{d}^{-1}$ ). The management of light intensity (Fx2ph.V2) throughout *P. gyrams* growth resulted in important gains in productivity for Fx and TCar, ranking the Fx2ph.V2 as the second and first most productive assay, respectively. Thus, the reduction from  $700$  to  $150 \mu\text{mol photons m}^{-2} \text{s}^{-1}$  in the last 2 days of growth can be seen as an interesting strategy for the

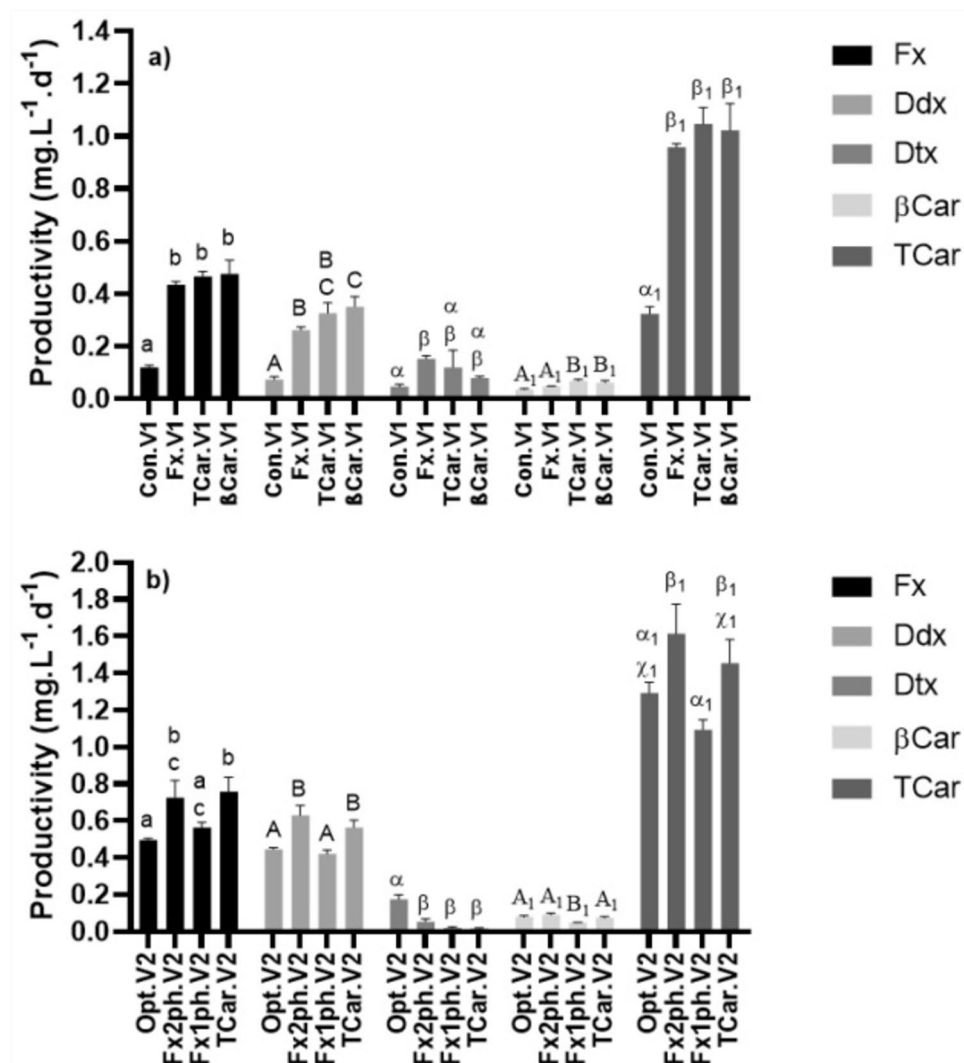


**Figure 3.** Volumetric productivities of the carotenoids (fucoxanthin, Fx; diadinoxanthin, Ddx; diatoxanthin, Dtx;  $\beta$ -carotene,  $\beta$ Car; total carotenoids, TCar),  $\text{mg L}^{-1} \text{d}^{-1}$ , of *P. gyrams* grown in validation conditions V1 (a) and V2 (b). In V1, was evaluated the Walne's medium (Con) and the maximized conditions for accumulation of fucoxanthin (Fx),  $\beta$ -carotene ( $\beta$ Car), and the sum of all carotenoids analyzed (TCar). In V2 (b) was assessed the optimized growth conditions for *P. gyrams*' biomass production (Opt) and the maximized growth conditions for TCar and fucoxanthin:  $150 \mu\text{mol photons m}^{-2} \text{s}^{-1}$  during the entire growth (Fx1ph) or using  $700 \mu\text{mol photons m}^{-2} \text{s}^{-1}$  for the first 8 days and  $150 \mu\text{mol photons m}^{-2} \text{s}^{-1}$  for the last 2 days (Fx2ph). Bars with different superscript letters are significantly different ( $p < 0.05$ ).

maximization of *P. gyrans*' biomass production, along with higher productivity for the biologically important carotenoids.

Looking at the pigment fucoxanthin, its maximum productivity value achieved with *P. gyrans* ( $0.759 \text{ mg L}^{-1} \text{ d}^{-1}$ ) is within the range described for other species that were studied as a fucoxanthin source, such as *Chaetoceros muelleri* ( $0.072 \text{ mg L}^{-1} \text{ d}^{-1}$ )<sup>45</sup>, *P. tricornutum* ( $0.041\text{--}2.3 \text{ mg L}^{-1} \text{ d}^{-1}$ )<sup>36,45</sup>, but on the other hand, it falls short of the productivity described for *Tisochrysis lutea* ( $4.71 \text{ mg L}^{-1} \text{ d}^{-1}$ )<sup>58</sup>. Although fucoxanthin productivity of *P. gyrans* is below some of the values recorded for *P. tricornutum* and *T. lutea*, it must be regarded as a promising alternative source of fucoxanthin. In particular, *Pavlova* species have some interesting characteristics, namely: a high content of omega-3 fatty acids; the absence of a rigid cell wall, which enhances their digestibility; and a perfectly balanced ratio between essential and non-essential amino acids, which makes them a complete source of bioactives for further application at industrial scale and as a valuable new ingredient for human consumption.

## Conclusion

In this work, a multivariate approach was implemented to identify the significant growth parameters on carotenoids' composition of *P. gyrans* ( $p < 0.10$ ). Fx content was mainly affected by the light intensity and  $\text{NaNO}_3$ , whereas TCar content was influenced by light intensity,  $\text{NaNO}_3$ , salinity, cobalt, and iron. The manipulation of the key abiotic factors proved successful due to the generalized increase in Fx and TCar. The highest Fx ( $6.153 \text{ mg g}^{-1} \text{ DW}$ ) and TCar ( $11.794 \text{ mg g}^{-1} \text{ DW}$ ) contents were achieved in the same experiment, in which the key variables were set to increase the total carotenoids content.

## Data availability

Data is available upon reasonable request through the following email: [jfilipemaciel@ceb.uminho.pt](mailto:jfilipemaciel@ceb.uminho.pt).

Received: 6 February 2024; Accepted: 8 July 2024

Published online: 26 July 2024

## References

- Frank, H. A. & Cogdell, R. J. Light capture in photosynthesis. In *Comprehensive Biophysics* Vol. 8 (ed. Egelman, E. H.) 94–114 (Elsevier, 2012).
- Bogacz-Radomska, L. & Harasym, J.  $\beta$ -Carotene-properties and production methods. *Food Qual. Saf.* **2**, 69–74 (2018).
- Mathews-Roth, M. M., Wilson, T., Fujimori, E. & Krinsky, N. I. Carotenoid chromophore length and protection against photosensitization. *Photochem. Photobiol.* **19**, 217–222 (1974).
- Hirayama, O., Nakamura, K., Hamada, S. & Kobayasi, Y. Singlet oxygen quenching ability of naturally occurring carotenoids. *Lipids* **29**, 149–150 (1994).
- BCC Research. Carotenoids Market Size, Share & Growth Analysis Report. <https://www.bccresearch.com/market-research/food-and-beverage/the-global-market-for-carotenoids.html> (2022).
- Aruldass, C. A., Dufossé, L. & Ahmad, W. A. Current perspective of yellowish-orange pigments from microorganisms- a review. *J. Clean. Prod.* **180**, 168–182 (2018).
- Capelli, B., Bagchi, D. & Cysewski, G. R. Synthetic astaxanthin is significantly inferior to algal-based astaxanthin as an antioxidant and may not be suitable as a human nutraceutical supplement. *Nutraceuticals* **12**, 145–152 (2013).
- Bojko, M. *et al.* Diadinoxanthin de-epoxidation as important factor in the short-term stabilization of diatom photosynthetic membranes exposed to different temperatures. *Plant Cell Environ.* **42**, 1270–1286 (2019).
- Bhattacharjya, R., Singh, P. K., Mishra, B., Saxena, A. & Tiwari, A. Phycoprospecting the nutraceutical potential of *Isochrysis* sp as a source of aquafeed and other high-value products. *Aquac. Res.* **52**, 2988–2995 (2021).
- Guedes, A. C., Amaro, H. M. & Malcata, F. X. Microalgae as sources of carotenoids. *Mar. Drugs* **9**, 625–644 (2011).
- Lamers, P. P. *et al.* Carotenoid and fatty acid metabolism in light-stressed *Dunaliella salina*. *Biotechnol. Bioeng.* **106**, 638–648 (2010).
- Chekanov, K. *et al.* Accumulation of astaxanthin by a new *Haematococcus pluvialis* strain BM1 from the white sea coastal rocks (Russia). *Mar. Drugs* **12**, 4504–4520 (2014).
- Hu, I.-C. Production of potential coproducts from microalgae. In *Biofuels from Algae* (eds Pandey, A. *et al.*) 345–358 (Elsevier, 2019).
- di Lena, G., Casini, I., Lucarini, M. & Lombardi-Boccia, G. Carotenoid profiling of five microalgae species from large-scale production. *Food Res. Int.* **120**, 810–818 (2019).
- Xi, Y., Wang, J., Chu, Y., Chi, Z. & Xue, S. Effects of different light regimes on *Dunaliella salina* growth and  $\beta$ -carotene accumulation. *Algal. Res.* **52**, 102111 (2020).
- Fradique, M. *et al.* *Isochrysis galbana* and *Diacronema vlikiianum* biomass incorporation in pasta products as PUFA's source. *LWT - Food Sci. Technol.* **50**, 312–319 (2013).
- Robertson, R. C. *et al.* An assessment of the techno-functional and sensory properties of yoghurt fortified with a lipid extract from the microalga *Pavlova lutheri*. *Innov. Food Sci. Emerg. Technol.* **37**, 237–246 (2016).
- Tibbetts, S. M. & Patelakis, S. J. J. Apparent digestibility coefficients (ADCs) of intact-cell marine microalgae meal (*Pavlova* sp. 459) for juvenile Atlantic salmon (*Salmo salar* L.). *Aquaculture* **546**, 737236 (2022).
- Shah, S. M. U., Ahmad, A., Othman, M. F. & Abdullah, M. A. Enhancement of Lipid Content in *Isochrysis Galbana* and *Pavlova Lutheri* Using Palm Oil Mill Effluent as an Alternative Medium. *Chem. Eng. Trans.* **37**, 733–738 (2014).
- Fernandes, T., Martel, A. & Cordeiro, N. Exploring *Pavlova pinguis* chemical diversity: A potentially novel source of high value compounds. *Sci. Rep.* **10**, 1–11 (2020).
- van Lenning, K. *et al.* Pigment signatures and phylogenetic relationships of the Pavlovophyceae (Haptophyta). *J. Phycol.* **39**, 379–389 (2003).
- Hitoe, S. & Shimoda, H. Seaweed fucoxanthin supplementation improves obesity parameters in mildly obese Japanese subjects. *Funct. Foods Health Dis.* **7**, 246–262 (2017).
- Lopes, F. G. *et al.* Anti-cancer effects of fucoxanthin on human glioblastoma cell line. *Anticancer Res.* **40**, 6799–6815 (2020).
- Zhang, Y. *et al.* Fucoxanthin ameliorates hyperglycemia, hyperlipidemia and insulin resistance in diabetic mice partially through IRS-1/PI3K/Akt and AMPK pathways. *J. Funct. Foods* **48**, 515–524 (2018).
- Maciel, F. *et al.* Optimization of *Pavlova gyrans* biomass production and the fatty acid profile using a two-step approach. *Sustain. Food Technol.* **1**, 850–862 (2023).
- Andersen, R. A. *Algal Culturing Techniques* (Elsevier Academic Press, 2005).

27. Rodrigues, M. I. & Iemma, A. F. *Experimental Design and Process Optimization* (CRC Press, 2014).
28. Sanz, N., García-Blanco, A., Gavalás-Olea, A., Loures, P. & Garrido, J. L. Phytoplankton pigment biomarkers: HPLC separation using a pentafluorophenyl octadecyl silica column. *Methods Ecol. Evol.* **6**, 1199–1209 (2015).
29. Zapata, M. & Garrido, L. Influence of injection conditions in reversed-phase high-performance liquid chromatography of chlorophylls and carotenoids. *Chromatographia* **31**, 589–594 (1991).
30. Zapata, M. *et al.* Photosynthetic pigments in 37 species (65 strains) of Haptophyta: Implications for oceanography and chemotaxonomy. *Mar. Ecol. Prog. Ser.* **270**, 83–102 (2004).
31. Fawley, M. W., Morton, S. J., Stewart, K. D. & Mattox, K. R. Evidence for a common evolutionary origin of light-harvesting fucoxanthin chlorophyll *a/c*-protein complexes of Pavlova gyrans (Prymnesiophyceae) and Phaeodactylum tricorneratum (Bacillariophyceae). *J. Phycol.* **23**, 377–381 (1987).
32. Guihéneuf, F. & Stengel, D. B. Interactive effects of light and temperature on pigments and n-3 LC-PUFA-enriched oil accumulation in batch-cultivated Pavlova lutheri using high-bicarbonate supply. *Algal Res.* **23**, 113–125 (2017).
33. Seoane, S., Zapata, M. & Orive, E. Growth rates and pigment patterns of haptophytes isolated from estuarine waters. *J. Sea Res.* **62**, 286–294 (2009).
34. Mckew, B. A. *et al.* The trade-off between the light-harvesting and photoprotective functions of fucoxanthin-chlorophyll proteins dominates light acclimation in Emiliania huxleyi (clone CCMP 1516). *New Phytol.* **200**, 74–85 (2013).
35. Kanamoto, A., Kato, Y., Yoshida, E., Hasunuma, T. & Kondo, A. Development of a method for fucoxanthin production using the haptophyte marine microalga pavlova sp. OPMS 30543. *Mar. Biotechnol.* **23**, 331–341 (2021).
36. McClure, D. D., Luiz, A., Gerber, B., Barton, G. W. & Kavanagh, J. M. An investigation into the effect of culture conditions on fucoxanthin production using the marine microalgae Phaeodactylum tricorneratum. *Algal Res.* **29**, 41–48 (2018).
37. Xia, S. *et al.* Production, characterization, and antioxidant activity of fucoxanthin from the marine diatom Odontella aurita. *Mar. Drugs* **11**, 2667–2681 (2013).
38. Fernandes, T. & Cordeiro, N. High-value lipids accumulation by Pavlova pinguis as a response to nitrogen-induced changes. *Biomass Bioenergy* **158**, 103641 (2022).
39. Longworth, J., Wu, D., Huete-Ortega, M., Wright, P. C. & Vaidyanathan, S. Proteome response of Phaeodactylum tricorneratum, during lipid accumulation induced by nitrogen depletion. *Algal Res.* **18**, 213–224 (2016).
40. Li, Q., You, J., Qiao, T., Zhong, D. & Yu, X. Sodium chloride stimulates the biomass and astaxanthin production by Haematococcus pluvialis via a two-stage cultivation strategy. *Bioresour. Technol.* **344**, 126214 (2022).
41. Ren, Y., Sun, H., Deng, J., Huang, J. & Chen, F. Carotenoid production from microalgae: Biosynthesis, salinity responses and novel biotechnologies. *Mar. Drugs* **19**, 713 (2021).
42. Fazeli, M. R., Tofghi, H., Samadi, N. & Jamalifar, H. Effects of salinity on  $\beta$ -carotene production by Dunaliella tertiolecta DCCBC26 isolated from the Urmia salt lake, north of Iran. *Bioresour. Technol.* **97**, 2453–2456 (2006).
43. Campenni, L. *et al.* Carotenoid and lipid production by the autotrophic microalga Chlorella protothecoides under nutritional, salinity, and luminosity stress conditions. *Appl. Microbiol. Biotechnol.* **97**, 1383–1393 (2013).
44. Mehariya, S., Plöhn, M., Leon-Vaz, A., Patel, A. & Funk, C. Improving the content of high value compounds in Nordic Desmodesmus microalgal strains. *Bioresour. Technol.* **359**, 127445 (2022).
45. Ishika, T. *et al.* Halo-adapted microalgae for fucoxanthin production: Effect of incremental increase in salinity. *Algal Res.* **28**, 66–73 (2017).
46. Rout, G. R. & Sahoo, S. Role of iron in plant growth and metabolism. *Rev. Agric. Sci.* **3**, 1–24 (2015).
47. Naumann, B., Stauber, E. J., Busch, A., Sommer, F. & Hippler, M. N-terminal processing of Lhca3 is a key step in remodeling of the photosystem I-light-harvesting complex under iron deficiency in Chlamydomonas reinhardtii. *J. Biol. Chem.* **280**, 20431–20441 (2005).
48. Kosakowska, A., Lewandowska, J., Ston, J. & Burkiewicz, K. Qualitative and quantitative composition of pigments in Phaeodactylum tricorneratum (Bacillariophyceae) stressed by iron. *BioMetals* **17**, 45–52 (2004).
49. Yamamoto, H. Y. & Bassi, R. Carotenoids: Localization and Function. in *Oxygenic Photosynthesis: The Light Reactions. Advances in Photosynthesis and Respiration* vol. 4 539–563 (Springer, 1996).
50. Hu, X., Wei, X., Ling, J. & Chen, J. Cobalt: An essential micronutrient for plant growth?. *Front Plant. Sci.* **12**, 768523 (2021).
51. Li, M. *et al.* Cobalt and manganese stress in the microalga Pavlova viridis (Prymnesiophyceae): Effects on lipid peroxidation and antioxidant enzymes. *J. Environ. Sci.* **19**, 1330–1335 (2007).
52. Latowski, D., Kuczyńska, P. & Strzałka, K. Xanthophyll cycle - a mechanism protecting plants against oxidative stress. *Redox. Rep.* **16**, 78–90 (2011).
53. Bhosale, P. Environmental and cultural stimulants in the production of carotenoids from microorganisms. *Appl. Microbiol. Biotechnol.* **63**, 351–361 (2004).
54. El-Sheekh, M., El-Naggar, A., Osman, M. & El-Mazaly, E. Effect of cobalt on growth, pigments and the photosynthetic electron transport in Monoraphidium minutum and Nitzschia perminuta. *Braz. J. Plant Physiol* **15**, 159–166 (2003).
55. Varshney, P., Sohoni, S., Wangikar, P. P. & Beardall, J. Effect of high CO<sub>2</sub> concentrations on the growth and macromolecular composition of a heat- and high-light-tolerant microalga. *J. Appl. Phycol.* **28**, 2631–2640 (2016).
56. Enriquez, M. M. *et al.* Direct determination of the excited state energies of the xanthophylls diadinoxanthin and diatoxanthin from Phaeodactylum tricorneratum. *Chem. Phys. Lett.* **493**, 353–357 (2010).
57. Fernandes, T. & Cordeiro, N. Effects of phosphorus-induced changes on the growth, nitrogen uptake, and biochemical composition of Pavlova pinguis and Hemiselmis cf. andersenii. *J. Appl. Phycol.* **34**, 757–775 (2022).
58. Gao, F., Sá, M., Cabanelas, I. T. D., Wijffels, R. H. & Barbosa, M. J. Improved fucoxanthin and docosahexaenoic acid productivities of a sorted self-settling Tisochrysis lutea phenotype at pilot scale. *Bioresour. Technol.* **325**, 124725 (2021).

## Acknowledgements

This study was supported by the Portuguese Foundation for Science and Technology (FCT) under the scope of the strategic funding of UIDB/04469/2020 unit and by LABELS—Associate Laboratory in Biotechnology, Bioengineering and Microelectromechanical Systems, LA/P/0029/2020. This work was financially supported by “Pacto da Bioeconomia azul” (Project No. C644915664-00000026) within the WP5 Algae Vertical, funded by Next Generation EU European Fund and the Portuguese Recovery and Resilience Plan (PRR), under the scope of the incentive line “Agendas for Business Innovation” through the funding scheme C5—Capitalization and Business Innovation. Filipe Maciel acknowledges the FCT for his fellowship (SFRH/BD/133005/2017; COVID/BD/152455/2022). Pedro Geada acknowledges FCT for the Junior Research contract obtained under the scope of the Scientific Stimulus Employment with the reference 2022.00930.CEECIND (<https://doi.org/10.54499/2022.00930.CEECIND/CP1718/CT0023>).

### Author contributions

F.M.: Conceptualization; Data curation; Formal analysis; Investigation; Methodology; Visualization; Writing—original draft; Writing—review & editing. P.B.: Conceptualization; Formal analysis; Investigation; Methodology; Writing—review & editing. P.G.: Conceptualization; Writing—review & editing. J.T.: Conceptualization; Funding acquisition; Resources; Writing—review & editing. J.S.: Conceptualization; Resources; Supervision; Writing—review & editing. A.V.: Conceptualization; Funding acquisition; Project administration; Resources; Supervision; Writing—review & editing.

### Competing interests

The authors declare no competing interests.

### Additional information

**Supplementary Information** The online version contains supplementary material available at <https://doi.org/10.1038/s41598-024-66986-y>.

**Correspondence** and requests for materials should be addressed to P.G.

**Reprints and permissions information** is available at [www.nature.com/reprints](http://www.nature.com/reprints).

**Publisher's note** Springer Nature remains neutral with regard to jurisdictional claims in published maps and institutional affiliations.



**Open Access** This article is licensed under a Creative Commons Attribution 4.0 International License, which permits use, sharing, adaptation, distribution and reproduction in any medium or format, as long as you give appropriate credit to the original author(s) and the source, provide a link to the Creative Commons licence, and indicate if changes were made. The images or other third party material in this article are included in the article's Creative Commons licence, unless indicated otherwise in a credit line to the material. If material is not included in the article's Creative Commons licence and your intended use is not permitted by statutory regulation or exceeds the permitted use, you will need to obtain permission directly from the copyright holder. To view a copy of this licence, visit <http://creativecommons.org/licenses/by/4.0/>.

© The Author(s) 2024